Supplement of Atmos. Chem. Phys., 25, 1121–1143, 2025
https://doi.org/10.5194/acp-25-1121-2025-supplement

Atmospheric Chemistry and Physics
Open Access
EGU

Supplement of

Urban ozone formation and sensitivities to volatile chemical products, cooking emissions, and NO_x upwind of and within two Los Angeles Basin cities

Chelsea E. Stockwell et al.

Correspondence to: Chelsea E. Stockwell (chelsea.stockwell@noaa.gov)

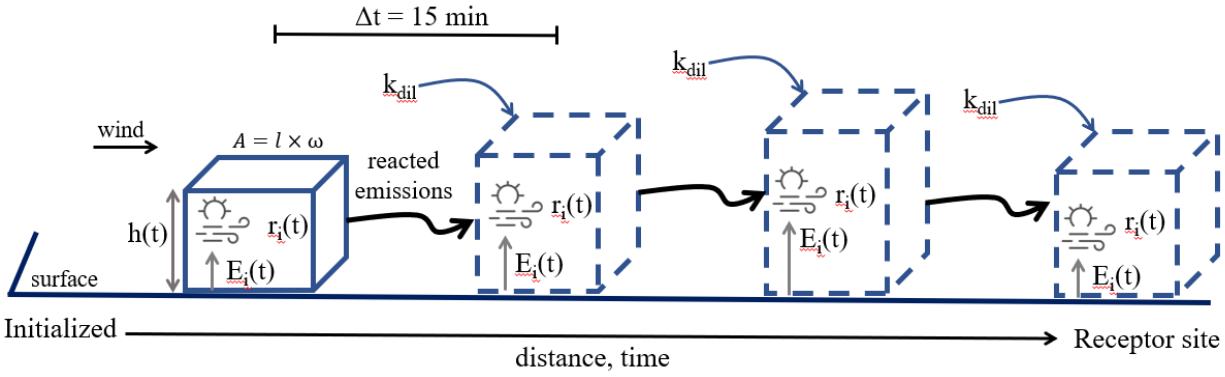

Figure S1. A simplified representation of the Lagrangian trajectory box model shows a well-mixed volume of air extending from the surface to the height of the boundary layer (h) within a defined area footprint (A). Each box model step is a coordinate (latitude, longitude, time) determined every 15 minutes along a trajectory path moving with the wind towards a receptor site. The starting mixing ratios in the initial box (solid box) or resulting from a previous model step (dashed box) are combined with a corresponding emission flux (E_i) from the surface. The contents are assumed to mix and chemically process (r_i) over the model step interval (Δt =15 min). The mass exchange with the air above and to the sides is represented by entrainment with background air (k_{dil}), which is estimated from changing boundary layer heights between model steps.

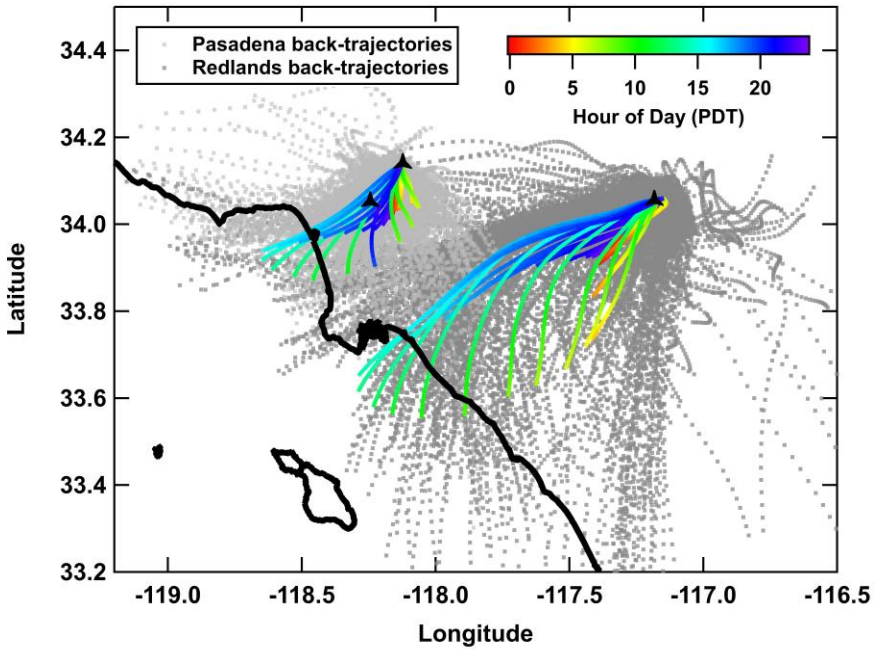

Figure S2. Each series of coordinates determined at 15 minute intervals from the FLEXPART-WRF backward trajectory analysis (grey dots). Twenty-five thousand particles (air parcels) were released hourly and traced backward from both Pasadena and Redlands to determine the dominant pathway (744 trajectories, each). The average trace is shown for each hourly release time and is colored by the local time of day.

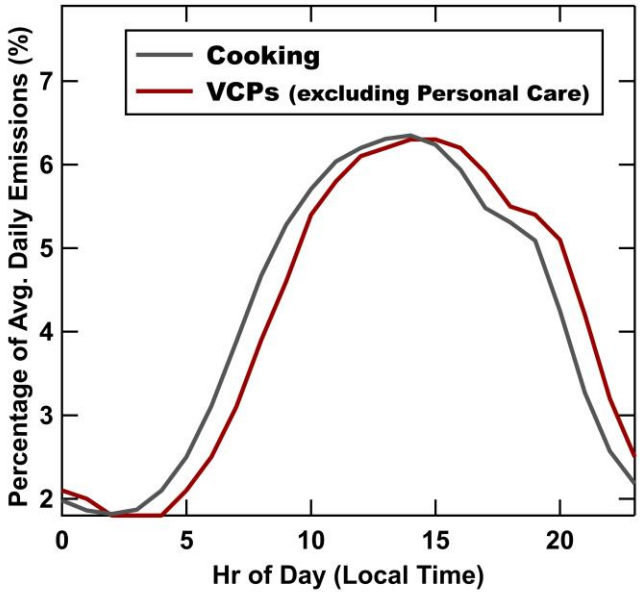

Figure S3. The temporal profile of cooking and VCP emissions as a percentage of average daily emissions used in the FIVE-VCP-NEI17NRT inventory. The cooking profile is taken from the 2017 National Emissions Inventory (NEI) commercial cooking temporal profile (code 26).

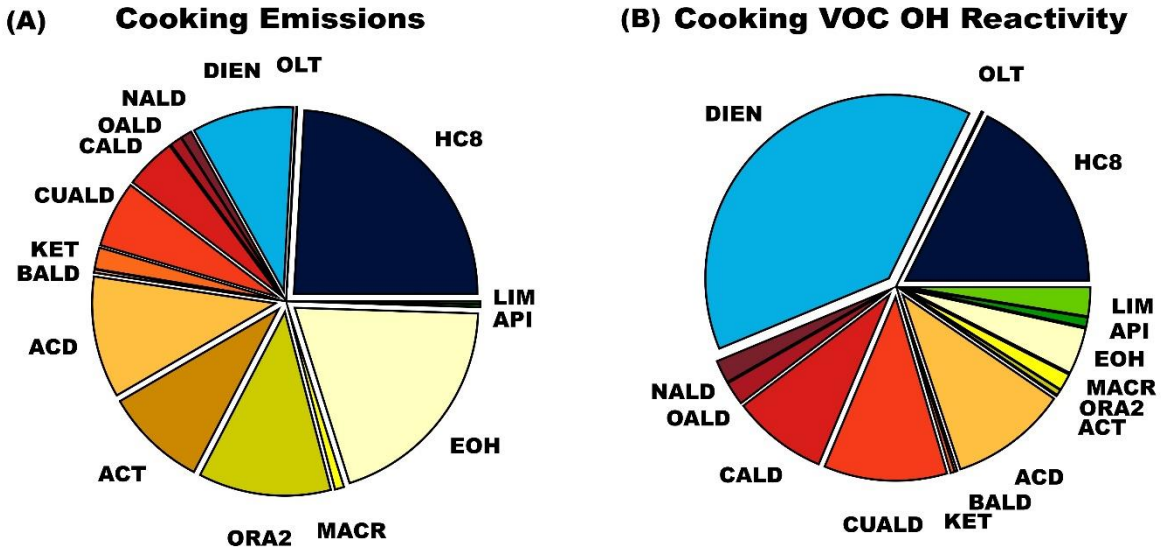

Figure S4. (A) The FIVE-VCP-NEI17NRT cooking emissions mapped to RACM2B-VCP species following the definition scheme outlined in Goliff et al. (2013). Chemical species added to the RACM2B-VCP mechanism include cooking saturated aldehydes (CALD), cooking unsaturated aldehydes (CUALD), octanal (OALD), and nonanal (NALD). (B) The lumped estimated VOC OH reactivity from cooking.

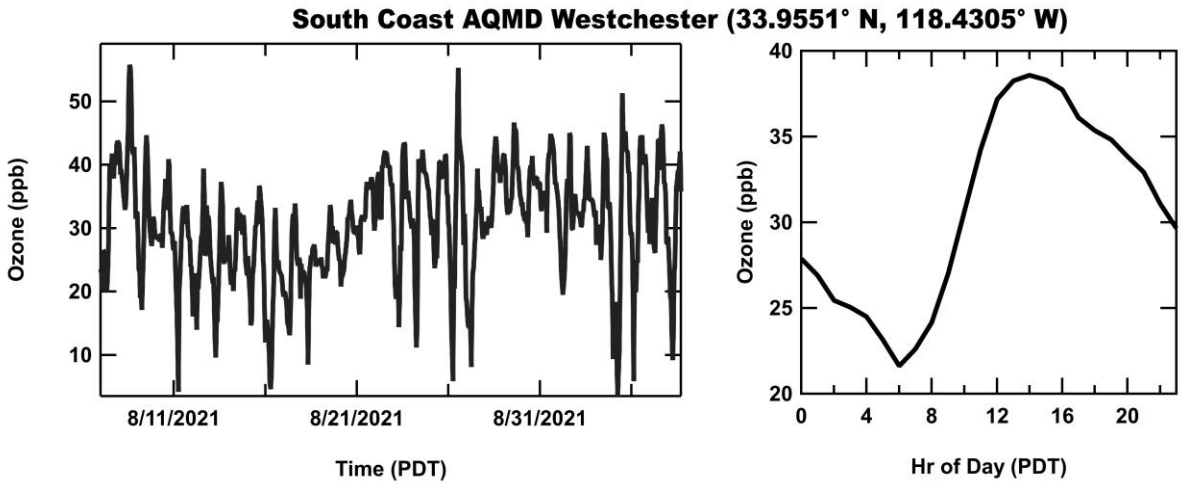

Figure S5. The O_3 time-series and diel profile from the South Coast Air Quality Management District (SCAQMD) Westchester site (33.9551° N, 118.4305° W) used as the initial O_3 mixing ratio in the model.

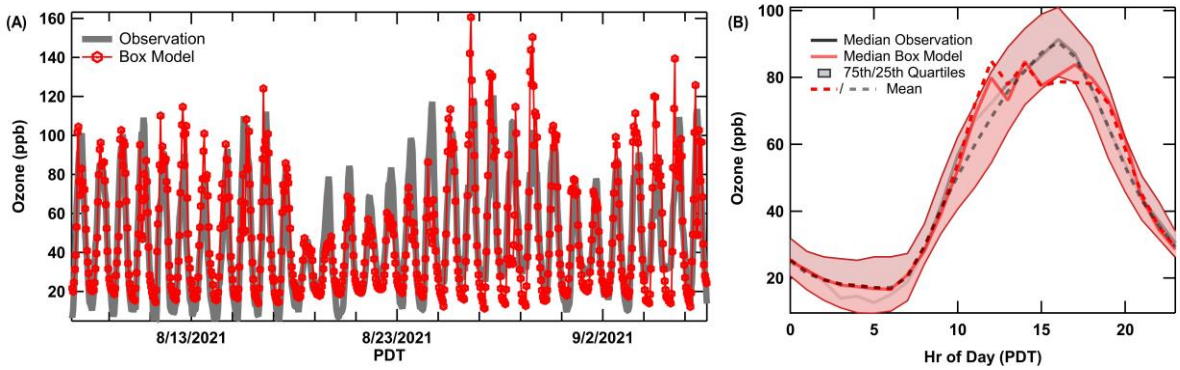

Figure S6. (A) The observed ozone time series (grey lines) overlaid with box model output (red markers) from 7 August – 7 September in Redlands, CA. (B) The median diel profile of modeled (red) and measured (grey) ozone in Redlands, CA. The mean is a dashed line and the median is marked by the solid. Shaded regions indicate the 75th- and 25th-quartile ranges.

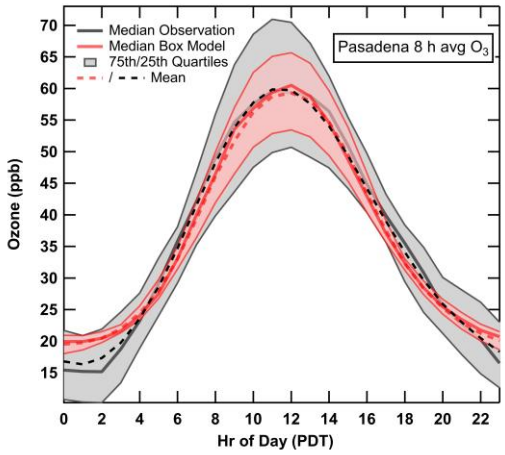

Figure S7. The median diel profile of the moving mean 8 h ozone (grey line) overlaid with box model output (red line) in Pasadena, CA. The mean is a dashed line and the median is marked by the solid. Shaded regions indicate the 75th- and 25th-quartile ranges.

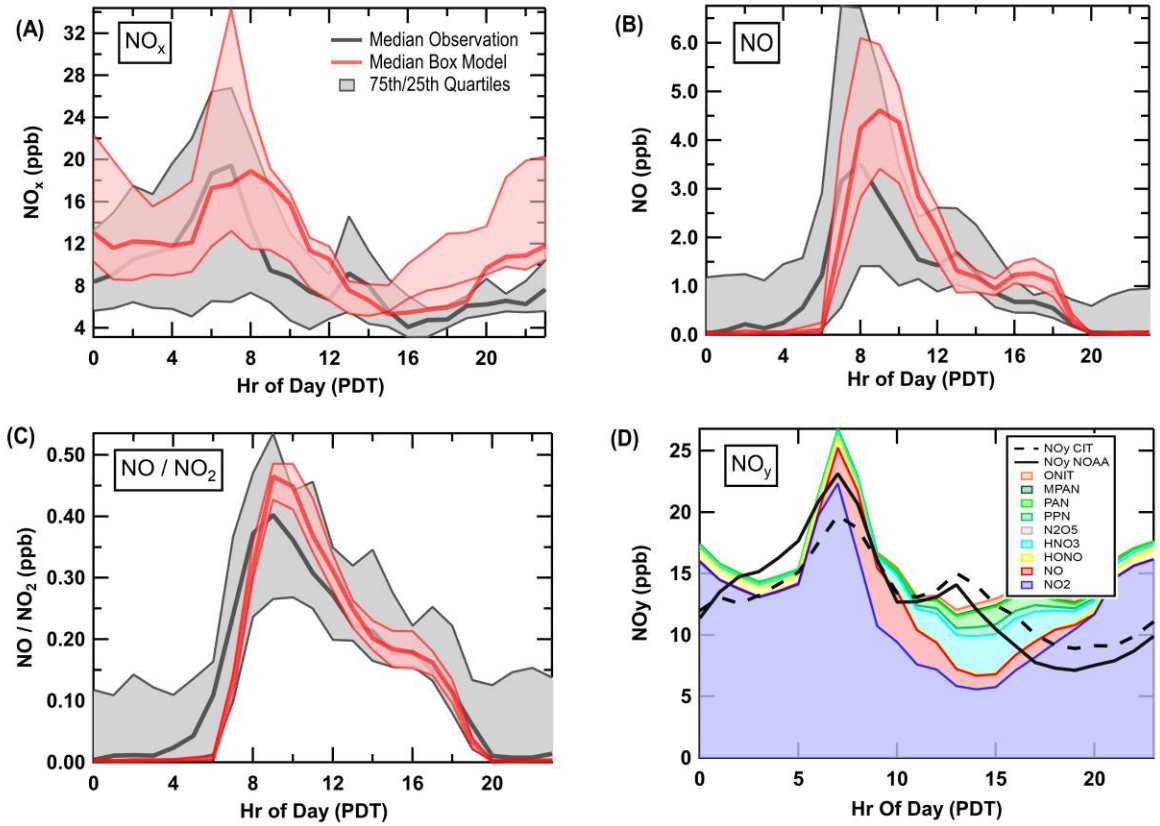

Figure S8. (A) The median diel profile NO_x (grey line) overlaid with box model output (red line). The mean is a dashed line and the median is marked by the solid line with shaded regions indicating the 75th- and 25th-quartile ranges. The median diel profile of (B) NO and (C) NO-to-NO_2 observations (grey) and model output (red). (D) The additive model output of speciated nitrogen compounds overlaid with the average NO_y measurements from the SUNVEx ground site (NO_y NOAA; solid black) and the Linde Laboratory (NO_y CIT; dashed black), both in Pasadena, CA.

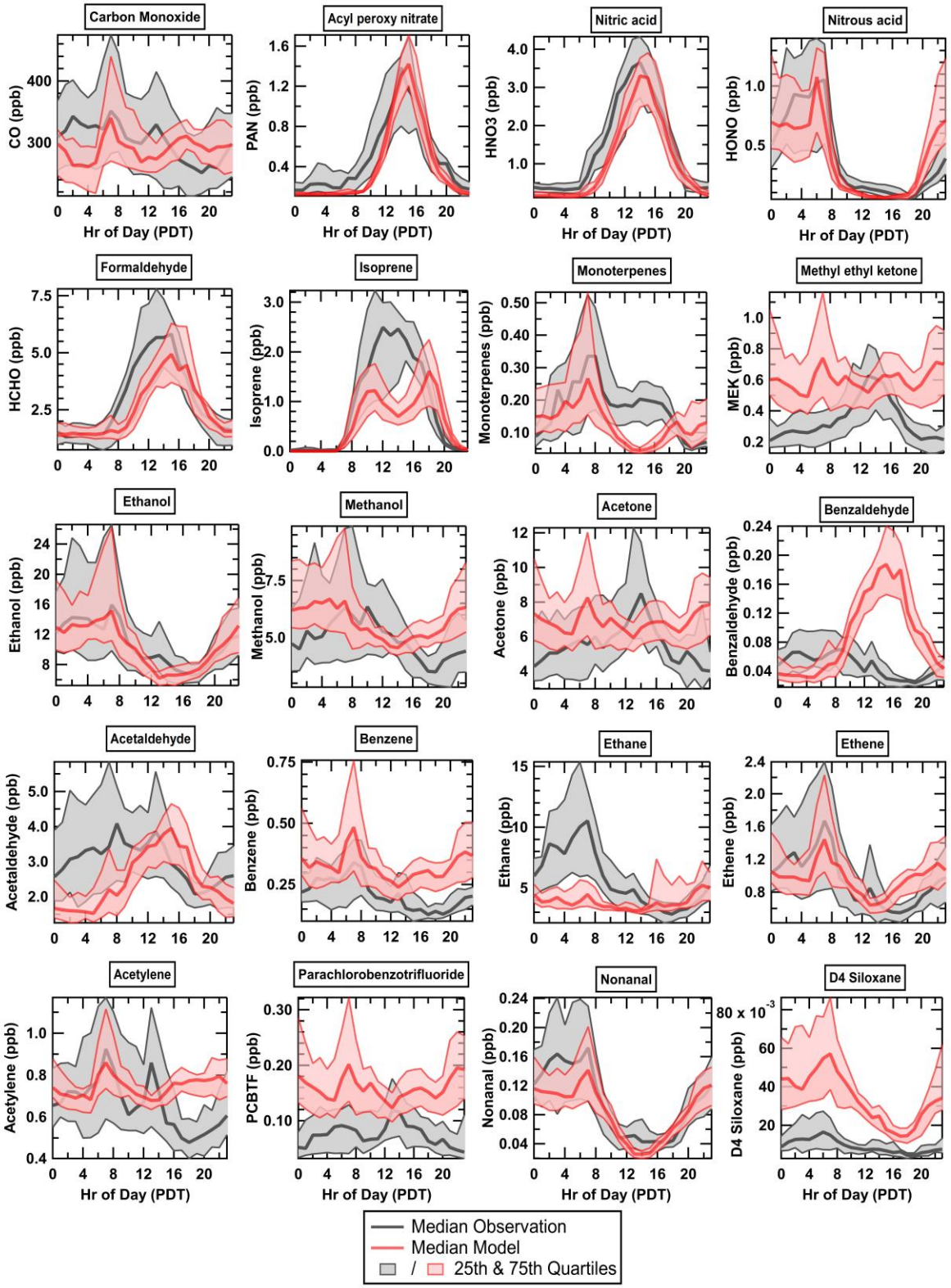

Figure S9. (A) The median diel profiles (grey) overlaid with box model results (red) for overlapping species modeled explicitly in the RACM2B-VCP mechanism scheme. The shaded regions indicate the 75th- and 25th-quartile ranges.

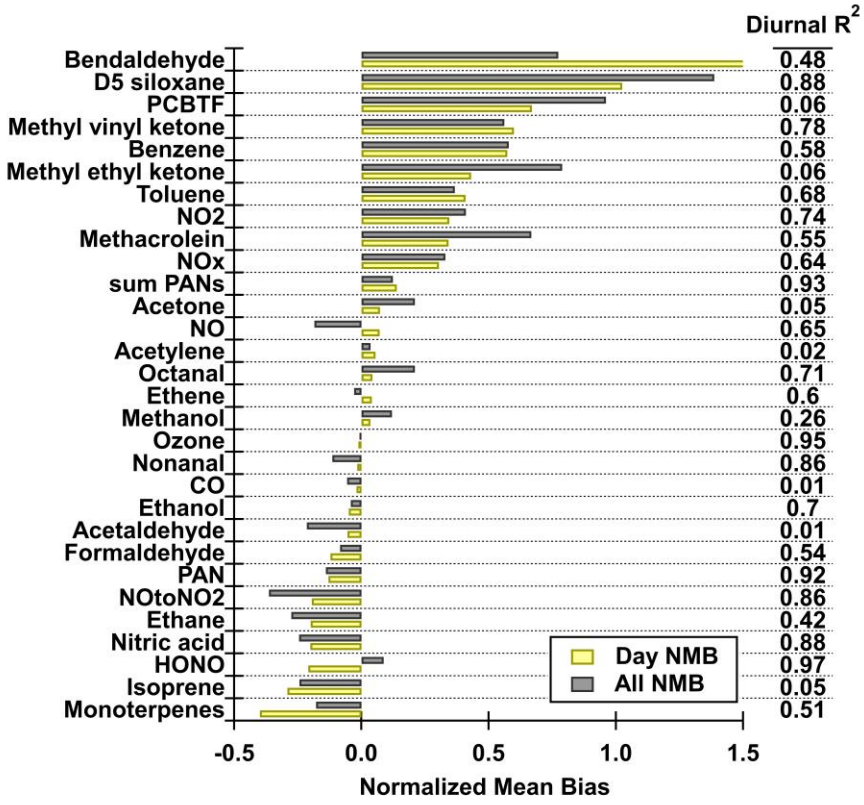

Figure S10. The box model normalized mean bias (NMB) and coefficient of determination (R^2) for explicit species in RACM2B-VCP that overlap with observations. The hourly NMB is calculated following Eq. (3) for all data (grey) and for daylight hours only (7:00-19:00 LT; yellow).

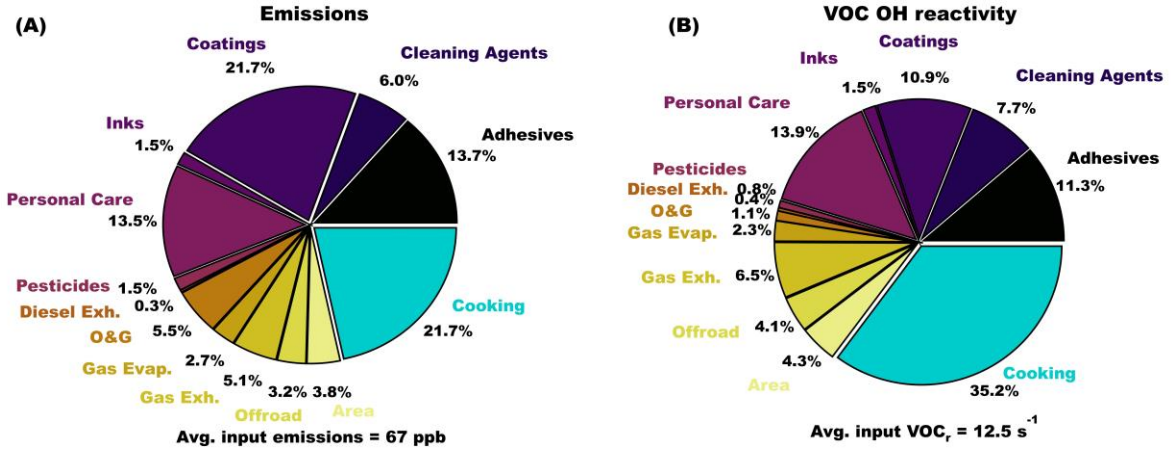

Figure S11. (A) The distribution of anthropogenic (A) VOC emissions and (B) VOC OH reactivity by emission source sector input into the model, averaged for arrival times in Pasadena between 12:00-15:00 LT.

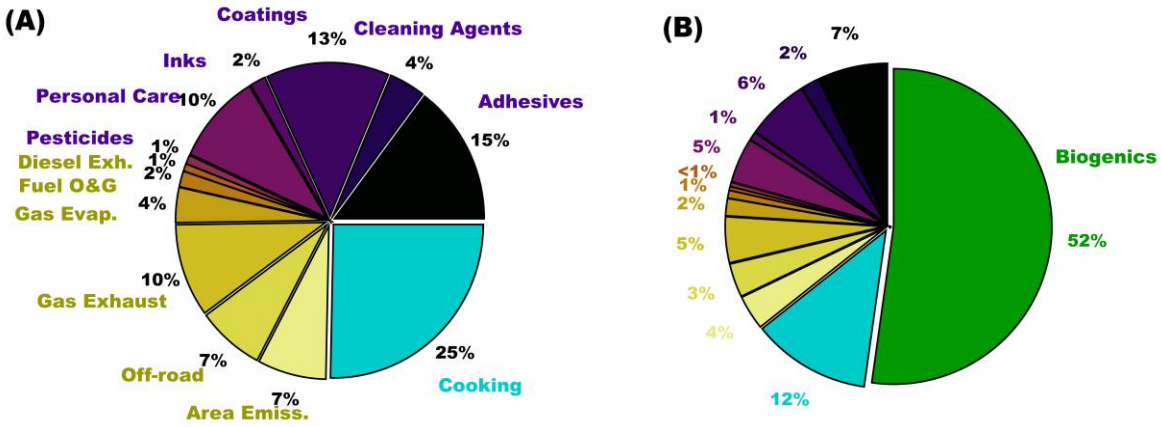

Figure S12. The fractional contribution to MDA8 ozone in Redlands, CA from: (A) anthropogenic VOC sources including VCPs (purple shading), fossil fuels (yellow shading), and cooking (blue) emissions. (B) anthropogenic plus biogenic VOCs.

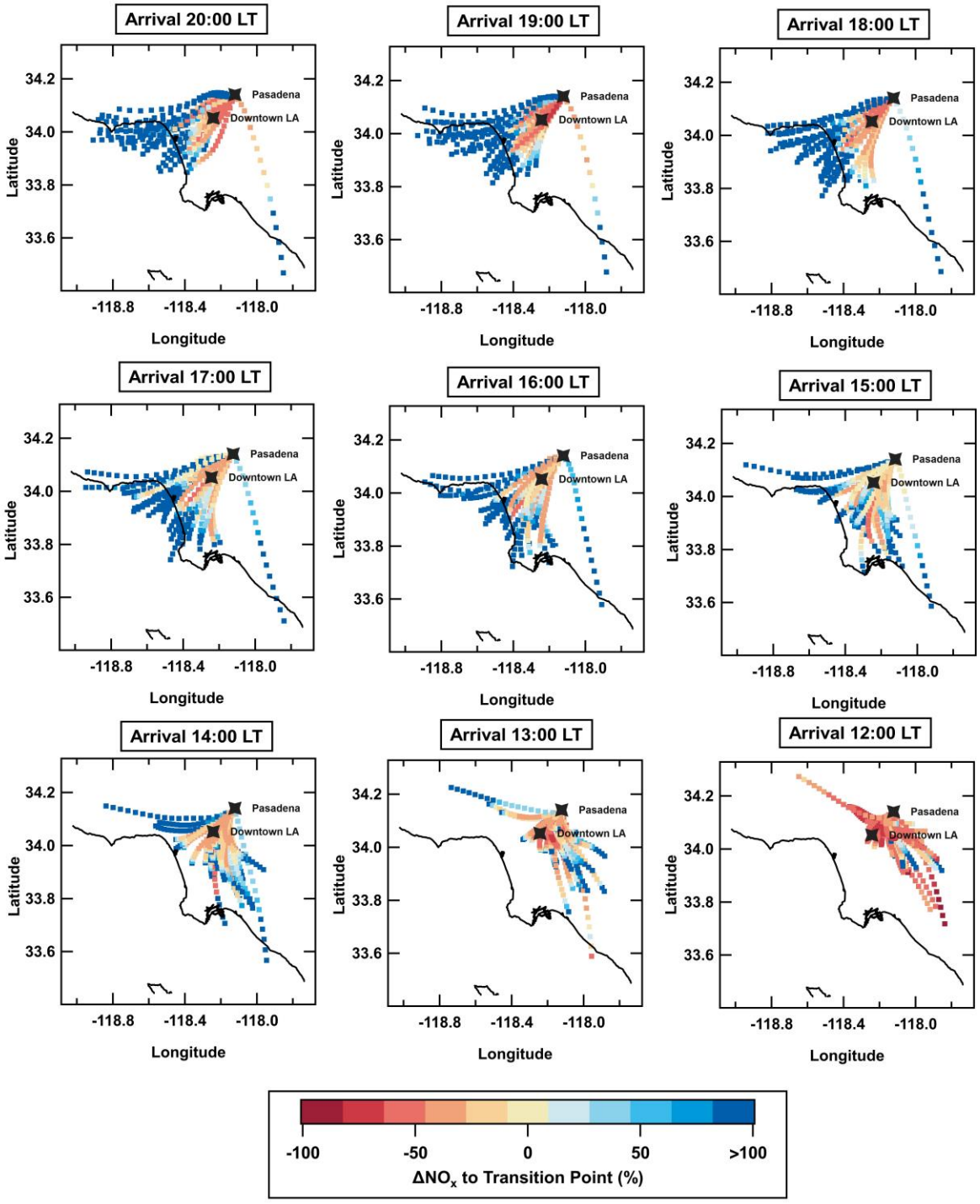

Figure S13. Trajectories arriving in Pasadena between 12:00-20:00 LT colored by the percent change in NO_x needed to transition between photochemical regimes. Warmer colors (-%) indicate the location is currently NO_x–saturated, while cooler (+%) is NO_x–limited.

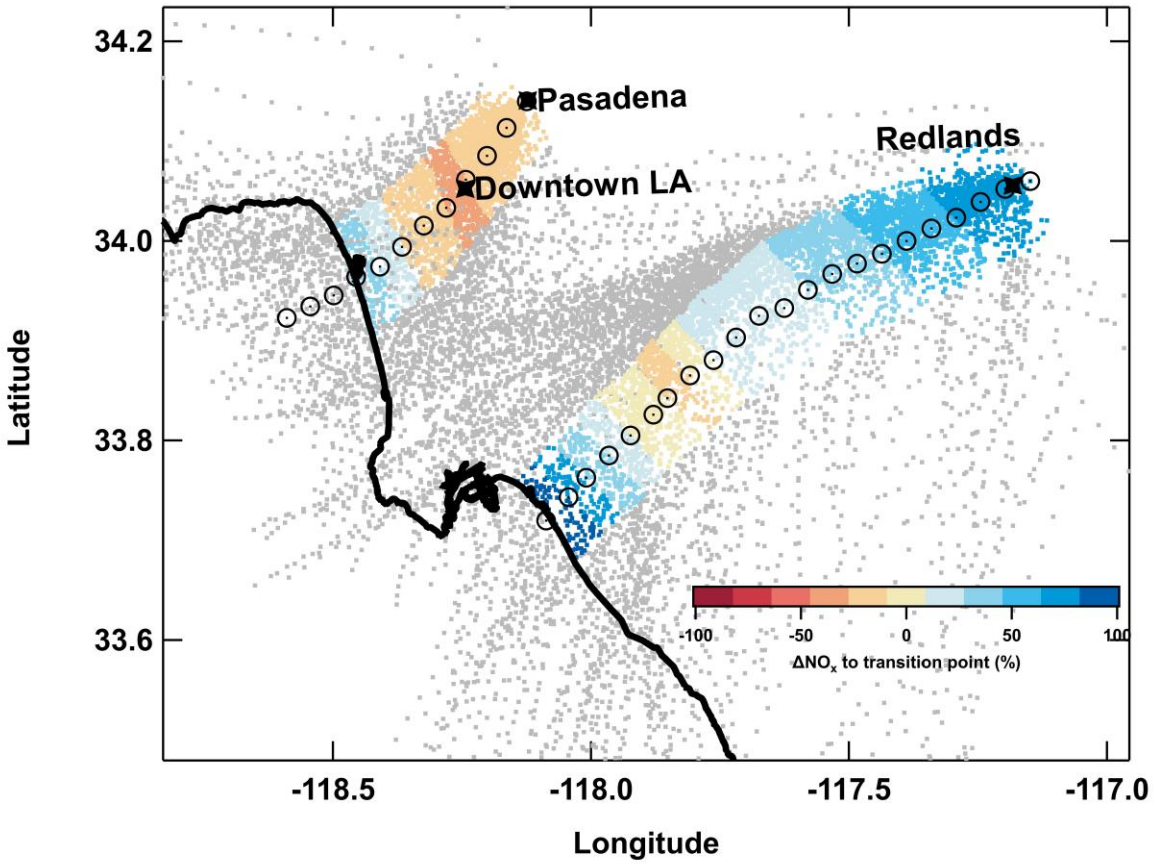

Figure S14. The trajectory paths to Pasadena and Redlands, CA averaged from 12:00-20:00 LT (black markers) overlaid with all backward trajectory parcel tracks (grey dots). The average change in NO_x emissions required to reach the transition within ± 8 km of each average trajectory path in 4 km segments is shown where warmer colors (-%) indicate the location is currently NO_x–saturated, while cooler (+%) is NO_x–limited.

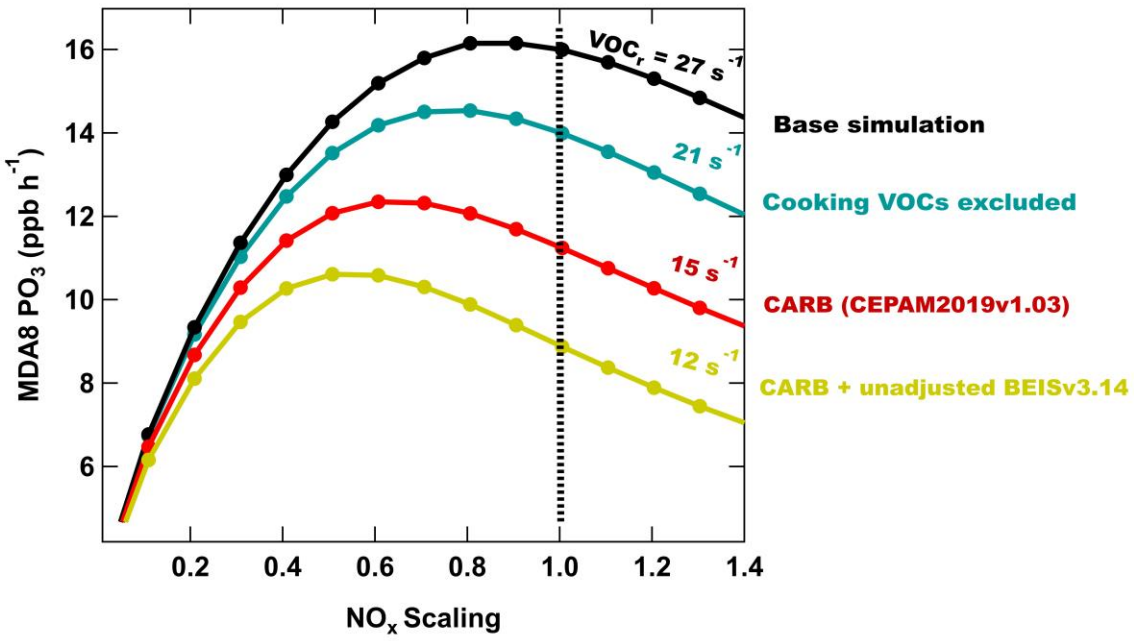

Figure S15. The change in the campaign average MDA8 ozone production rate (PO_3) as NO_x is scaled from its initial mixing ratio (hatched line) for the following scenarios: (1) base model simulations, (2) base emissions excluding cooking VOCs (blue), (3) emissions where VOCs were adjusted to better match the CARB-CEPAM inventory emissions (red), and (4) BVOCs scaled down to match the original BVOCs prescribed by the BEIS inventory coupled with WRF-Chem (yellow). PO_3 is defined by Supplemental Eq. (S1).

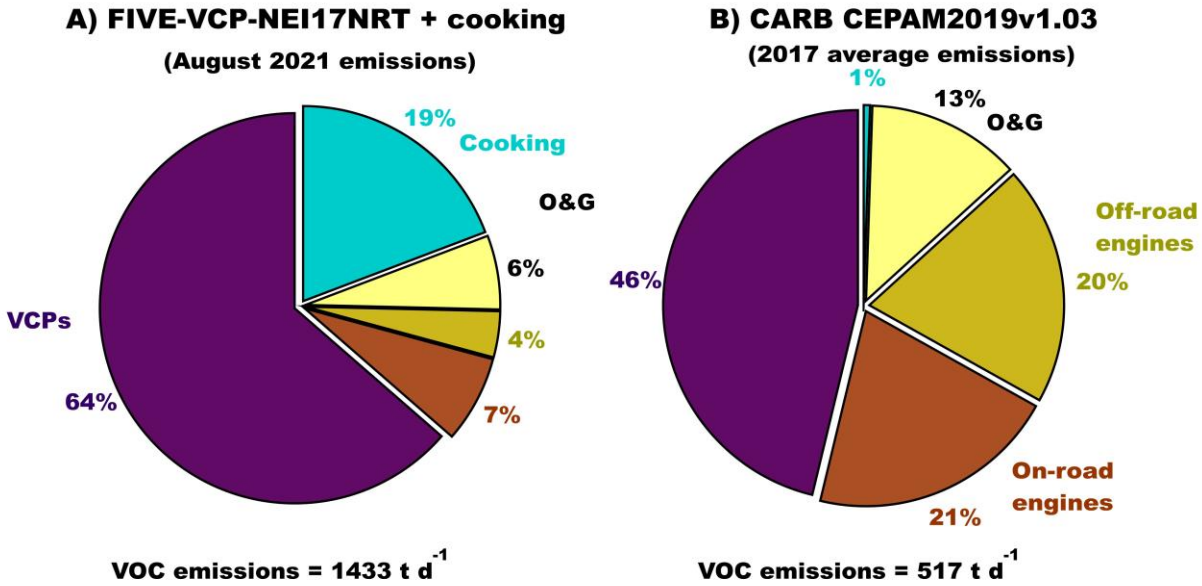

Figure S16. Distribution of VOC emissions in the South Coast Air Basin from the (A) FIVE-VCP-NEI17NRT inventory for August, 2021 and (B) CARB CEPAM2019v1.03 tool that represents annual emissions for 2017. Note: In the FIVE-VCP-NEI17NRT inventory base cooking emission estimates were used, and cooking ethanol was not adjusted to align with aircraft flux measurements as outlined in Section 2.2.2.

Species	Formula	WRF	RACM2B-VCP	Mass Fraction (base)	Mass Fraction (upper EOH)
Acetaldehyde	C2H4O	HC15	ACD	0.068	0.043
Ethanol	C2H6O	HC48	EOH	0.130	0.449
Acrolein	C3H4O	HC27	CUALD	0.006	0.004
Acetone / propanal	C3H6O	HC18	ACT	0.075	0.048
Acetic acid	C2H4O2	HC31	ORA2	0.068	0.043
Butenal	C4H6O	HC67	CUALD	0.006	0.004
Propanoic acid	C3H6O2	HC32	ORA2	0.011	0.007
Pentadienal	C5H6O	HC46	DIEN	0.039	0.024
Butenedial	C4H4O2	HC67	CUALD	0.004	0.002
Pentenal	C5H10O	HC67	CUALD	0.041	0.026
Pentanal	C5H10O	HC62	CALD	0.037	0.024
Buytrolactone	C4H6O2	HC20	KET	0.014	0.009
Hexadienal	C6H8O	HC46	DIEN	0.042	0.027
Pentanoic acid	C5H10O2	HC32	ORA2	0.004	0.002
Heptadienal	C7H10O	HC46	DIEN	0.004	0.003
Heptenal	C7H12O	HC67	CUALD	0.009	0.006
Heptanal	C7H14O	HC64	CALD	0.013	0.008
Octadienal	C8H12O	HC46	DIEN	0.013	0.008
Octenal	C8H14O	HC67	CUALD	0.011	0.007
Octanal	C8H16O	HC65	OALD	0.019	0.012
Heptanoic acid	C7H14O2	HC32	ORA2	0.001	0.000
Monoterpene	C10H16	HC11	0.5*LIM+0.5*API	0.010	0.006
Nondienal	C9H14O	HC46	DIEN	0.009	0.006
Nonenal	C9H16O	HC67	CUALD	0.004	0.002
Nonanal	C9H18O	HC66	NALD	0.020	0.013
Octanoicacid	C8H16O2	HC32	ORA2	0.002	0.002
Decatrienal	C10H14O	HC46	DIEN	0.014	0.009
Decadienal	C10H16O	HC46	DIEN	0.012	0.007
Decenal	C10H18O	HC67	CUALD	0.003	0.002
Decanal	C10H20O	HC68	CALD	0.004	0.003
Nonanoicacid	C9H18O2	HC32	ORA2	0.001	0.001
Undecenal	C11H22O	HC67	CUALD	0.001	0.001
Undecanal	C11H20O	HC68	CALD	0.002	0.001
Decenoicacid	C10H18O2	HC08	OLT	0.002	0.001
Decanoicacid	C10H20O2	HC32	ORA2	0.001	0.000
Tridecanal	C13H26O	HC68	CALD	0.002	0.001
Furfural	C5H4O2	HC68	CALD	0.005	0.003
C7H8O2	C7H8O2	HC32	ORA2	0.005	0.003
Benzaldehyde	C7H6O	HC17	BALD	0.004	0.003
C6H8O2	C6H8O2	HC32	ORA2	0.004	0.003

C6H10O2	C6H10O2	HC32	ORA2	0.016	0.010
C8H1002	C8H1002	HC32	ORA2	0.003	0.002
C8H12O2	C8H12O2	HC32	ORA2	0.003	0.002
C8H14O2	C8H14O2	HC32	ORA2	0.006	0.004
C9H14O2	C9H14O2	HC32	ORA2	0.002	0.001
C9H16O2	C9H16O2	HC32	ORA2	0.002	0.002
Unspeciated	NA	HC06	HC8	0.249	0.158

Table S1. The cooking speciation profile (mass fraction) determined by Coggon et al. (2024) mapped to the RACM2B-VCP mechanism.

Species	Reaction	Rate & Reaction coefficients
Saturated Aldehydes with C > 5	CALD+HO=0.19 HC5P+0.81 RCO3+H2O+OHR+OHVOC	7.23e-12*exp(410.0 / T)
	CALD+NO3=0.22 HC5P+0.78 RCO3+HNO3+PHNO3+LNOXHNO3	1.60E-14
	CALD+hv=HC5P+HO2+CO	JALD
Unsaturated Aldehydes with C > 5	CUALD+HO=0.53 MACP+0.47 UALP+OHR+OHVOC	8.0e-12*exp(380.0 / T)
	CUALD+NO3=MACP+HNO3+PHNO3+LNOXHNO3	3.40E-15
	CUALD+O3=0.902 MGLY+0.242 HCHO+0.238 HO+0.652 CO+0.098 RCO3+0.204 ORA1+0.14 HO2+0.144 H2O2	1.4e-15*exp(-2100.0 / T)
	CUALD+hv=0.5 MACP+0.175 RCO3+0.5 HCHO+0.325 ETHP+0.825 CO+HO2	JMACR
Octanal	OALD+hv=HC8P+HO2+CO	JALD
	OALD+HO=0.14 HC8P+0.86 RCO3+H2O+OHR+OHVOC	7.78e-12*exp(410.0 / T)
	OALD+NO3=0.2 HC8P+0.8 RCO3+HNO3+PHNO3+LNOXHNO3	1.70E-14
Nonanal	NALD+hv=HC8P+HO2+CO	JALD
	NALD+HO=0.15 HC8P+0.85 RCO3+H2O+OHR+OHVOC	8.08e-12*exp(410.0 / T)
	NALD+NO3=0.19 HC8P+0.81 RCO3+HNO3+PHNO3+LNOXHNO3	2.00E-14

Table S2. Added reactions for cooking saturated aldehydes (CALD), cooking unsaturated aldehydes (CUALD), octanal (OALD), and nonanal (NALD). Additional species identifiers can be found in Goliff et al. (2013).

RACM2B-VCP Species Name	Background concentration (ppb)
ACD	0.4
ACE	0.5
ACT	1.85
ALD	0.7
EOH	2
ETE	0.3
ETH	2.4
HC3	1.9
HC5	0.7
HC8	0.8
HCHO	0.8
MOH	3
TOL	0.1
CO	160-210
NO	0.2
NO2	1

Table S3. Background concentrations of CO, NO_x, and VOCs.

$$PO_3 = k_{HO_2+NO}[HO_2][NO] + \sum_i k_{RO_{2_i}+NO}\left[RO_{2_i}\right][NO] - k_{O1D+H_2O}[O1D][H_2O] - k_{OH+NO_2}[OH][NO_2] - k_{HO_2+O_3}[HO_2][O_3] - k_{OH+O_3}[OH][O_3] - k_{alkenes+O_3}[Alkenes][O_3] \quad \text{(S1)}$$

References

Coggon, M. M., Stockwell, C. E., Xu, L., Peischl, J., Gilman, J. B., Lamplugh, A., Bowman, H. J., Aikin, K., Harkins, C., Zhu, Q., Schwantes, R. H., He, J., Li, M., Seltzer, K., McDonald, B., and Warneke, C.: Contribution of cooking emissions to the urban volatile organic compounds in Las Vegas, NV, Atmos. Chem. Phys., 24, 4289-4304, 10.5194/acp-24-4289-2024, 2024.

Goliff, W. S., Stockwell, W. R., and Lawson, C. V.: The regional atmospheric chemistry mechanism, version 2, Atmospheric Environment, 68, 174-185, https://doi.org/10.1016/j.atmosenv.2012.11.038, 2013.